Attitude Determination and Control System Design for the CYGNSS MicroSatellite

Matthew Fritz, Joseph Shoer, Leena Singh, Tim Henderson
The Charles Stark Draper Laboratory
555 Technology Square, Cambridge, MA 02139
281.212.1130
mfritz@draper.com, jshoer@draper.com,
lsingh@draper.com, thenderson@draper.com

Jacob McGee, Randy Rose
South West Research Institute
6220 Culebra Road, San Antonio, TX
210.522.3315
jmcgee@swri.edu, RRose@swri.edu

Chris Ruf
Director, Space Physics Research Laboratory
Professor, Atmospheric, Oceanic and Space Sciences
University of Michigan
734.764.6561
cruf@umich.edu

***Abstract*—This paper presents the development of the attitude determination and control system design of the Cyclone Global Navigation Satellite System spacecraft. The CYGNSS constellation consists of eight small satellite observatories in 500 km circular orbits at an inclination of $35\,\mathrm{deg}$ released from a single launch platform. Each CYGNSS spacecraft will make frequent and accurate measurements of ocean surface winds throughout the life cycle of tropical storms and hurricanes with the objective to fundamentally improve gap-free coverage for hurricane forecast and monitoring. Realising this objective requires the spacecraft to accurately and reliably point its signal collection antennae in desired directions and hold its Earth relative attitude over long time durations to prescribed knowledge and point requirements. Indeed, the microsatellite ADCS regulates all spacecraft estimation and control functionality spanning detumbling; Sun acquisition and hold; pointing control and momentum-management over the micro-satellite lifetime to design requirements. This paper presents the ADCS hardware, software and algorithms used to control the spacecraft in all phases of CYGNSS operations and presents simulation based performance results of the closed-loop estimation and control systems.**

TABLE OF CONTENTS

1. INTRODUCTION

The Cyclone Global Navigation Satellite System (CYGNSS) mission consists of a constellation of eight 25kg microsatellite observatories in low Earth orbit being developed for space-based weather monitoring of tropical cyclones [1]. The eight microsatellites will be released from a single launch vehicle (LV) into an approximately circular 500km orbit at 35° inclination. With no onboard propellant or translation control actuation for orbit management, all on-orbit control post-separation is handled by the attitude determination and control system (ADCS) strategically leveraging environmental drag to effect the desired forces, thus capturing the constellation's desired orbital parameters. Indeed, with no thrusters, the microsatellite ADCS will be responsible for all spacecraft closed-loop functionality spanning stabilisation; Sun acquisition and hold; pointing control and momentum-management for all mission functions. This paper presents the ADCS sensor & actuator suite, architecture and algorithms used to control the spacecraft in all phases of on-orbit CYGNSS operations.

The CYGNSS spacecraft is a pyramidal structure with deployable solar arrays. The pyramidal faces enable the side panels to accommodate antennae for signal collection during science operations. Body mounted solar panels on three faces enable supplementary power collection during the mission when the microsat is oriented less Sun favourably. While the objective pointing attitudes of the microsatellite differ depending on the mission operational mode, the top deck with the main solar arrays defines its zenith face during Science operations when the antennae surfaces are maintained nadir pointed. Preferred wake and ram orientations are likewise imposed, see Fig. 1.

On-orbit operations, performance and endurance requirements have mandated the ADCS sensor and actuator suite as well as the ADCS concept of operations. The ADCS sensor suite comprises a magnetometer; a single-headed star tracker; a co-boresighted medium Sun sensor for operation during star tracker solar outages; and a top-deck mounted coarse Sun sensor (CSS) to aid in solar pointing the solar arrays. The ADCS actuator suite consists of three (3) torque rods and a reaction wheel triad assembly (RWA) suitably oriented to ensure that the central pyramidal axis is oriented along the microsat pitch rotation axis.

The spacecraft ADCS flight software must enable and support attitude estimation and control of the spacecraft in the following key operational configurations:

Rate Damp: ADCS must detumble the spacecraft after separation from the LV or in other loss-of-control phenomena into a despun state before transitioning into a Sun pointed attitude.

978-1-4799-5380-6/15/$31.00 ©2015 IEEE.

Only the magnetometer and torque rods are used in this mode to estimate and control effective rates.

Sun Point: After detumbling, the spacecraft must acquire and maintain an attitude with its solar arrays oriented towards the Sun. This is also the spacecraft's Safe mode of operations and is required to be performed with a minimum of sensors. A conical-scanning approach, leveraged from traditional radar pointing-&-tracking systems, sets up a spin-stabilised micro-satellite configuration with the solar arrays favourably Sun pointed in a dynamic torque equilibrium that can be reliably maintained with low control effort.

High-Drag Torque Equilibrium Attitude: Used both to realise the desired orbit as well as deorbit the spacecraft at its end-of-life, HDTEA is a fully attitude controlled configuration whereby the spacecraft pitches to project its largest effective drag surface area, i.e. its solar-arrays, along the velocity vector thus maximising the aerodynamic drag force on the satellite. A torque equilibrium attitude relative to the Earth and orbit-relative LVLH frame close to this maximum-projected aerodynamic-drag area configuration defines the desired attitude set-point for the HDTEA configuration. All sensors and actuators on the spacecraft are available for full-featured Kalman filter-based attitude estimation and closed-loop attitude control with momentum management.

Nadir Point: This is the desired attitude for science data collection on CYGNSS in addition to other spacecraft operations. In the nadir pointed configuration, the antenna deck of the spacecraft is oriented and maintained nadir pointed. As in the HDTEA configuration, all available sensors are available to the attitude determination system for attitude sensing as are all actuators for closed-loop pointing.

Specific features of the ADCS system on CYGNSS stem from the challenges of inserting reliability of operations into volume, power and space constrained small satellites of the cube satellite scale. Small spacecraft with relatively large area to volume ratios compared with large monolithic spacecraft incur relatively large disturbance forces and torques from aerodynamic and/or solar pressure effects due to their low ballistic coefficient. This calls for either more control authority - typically hard to achieve in volumetrically constrained systems - or novel operational concepts that leverage near-equilibrium stability configurations. Other similar small spacecraft have encountered such challenges, and defined with their own approaches to overcoming them; see references [2], [3] amongst many others.

CYGNSS is expected to launch in October 2016 and is currently in the early implementation stages with a protype engineering model being assembled and early flight software testing in progress.

This paper describes the attitude determination system (ADS) and attitude control system (ACS) objectives, design, architecture and algorithms in support of the spacecraft configurations summarised above and provide simulation-based data demonstrating expected performance and robustness of the ADCS in all the microsat modes.

2. SPACECRAFT LAYOUT AND FRAMES OF REFERENCE

CYGNSS is a pyramidal spacecraft with body-fixed solar panels on three faces (+X, -X, -Z) and two additional deployable solar arrays which fold onto each other over its -Z face for launch and orbit insertion. The $\pm X$ faces are the micro-satellite's ram and wake faces, respectively, when in its nominal nadir pointed configuration and will be referenced accordingly. Likewise, the $-Z$ deck with the largest solar arrays in their deployed state serves as its Zenith or anti-nadir face in this same nadir pointed configuration and will also be referenced accordingly.

The body-fixed vehicle frames as well as the nomenclature used in this paper to represent the orbit-referenced Local-Vertical-Local-Horizontal (LVLH) frames are shown in Fig. 1.

The LVLH frame +Z axis is pointed towards the centre of the Earth, the +Y axis is oriented along the orbit normal and the +X axis lies in the orbit-plane perpendicular to +Z in the direction of the velocity vector such that the three vectors define a right triad.

The spacecraft body frame aligns with the LVLH frame in our nadir pointed attitude configuration. The High-Drag TEA is another configuration in which the spacecraft must operate relative to the orbit-relative LVLH configuration. The HDTEA for CYGNSS corresponds to a pitch down of about 81 degrees, relative to the spacecraft's Y-axis along the orbit normal, pointing the vehicle -Z axis nearly along the LVLH +X presenting its maximum effective area for a high-drag flight.

Sun Point attitude is referenced relative to the Sun vector and orients the body -Z towards the Sun. This is a spin-stabilised mode about the body principal axis and thus only the Z axis is directionally stabilised. Detumble likewise is a rate regulation mode where no preferred attitude is sought.

3. CYGNSS ADCS MODES AND POINTING AND ATTITUDE ESTIMATION REQUIREMENTS

To stabilise the spacecraft in all the operational configurations defined for CYGNSS, ADCS has three principal operating modes defined: Rate Damp, Sun Point and LVLH hold. Detumble is effected via Rate Damp mode, while the HDTEA and Nadir Point configuration sequences are realised in LVLH hold mode with specific, fixed LVLH relative attitude set-points. Other intermediate LVLH relative pointing attitudes are also quite simply achieved with ADCS in LVLH and the LVLH relative pointing offset commanded as a desired quaternion and rate (likely 0 in any LVLH fixed pointing configuration) relative to the LVLH frame of reference.

Science performance related mission requirements on attitude knowledge and control requirements are largely imposed in the nadir pointed LVLH operations only. Here CYGNSS is required to be capable of estimating its attitude to within 2.2° per axis (3σ) of truth through the upto 22-minute Sun induced star tracker outages in its orbit when no star tracker aiding is available; it must also be able to control its pointing to within 5° per axis (3σ) of nadir alignment.

In the HDTEA pointing configuration, the only formal requirements specified are on pointing control whereby ADCS must be capable of controlling the spacecraft to within 5° in roll and 10° per pitch and yaw axes (3σ) relative to the desired maximum drag attitude specified relative to the LVLH frame.

Safety, deployment and operational requirements stipulated that the CYGNSS ADCS system must detumble the space-

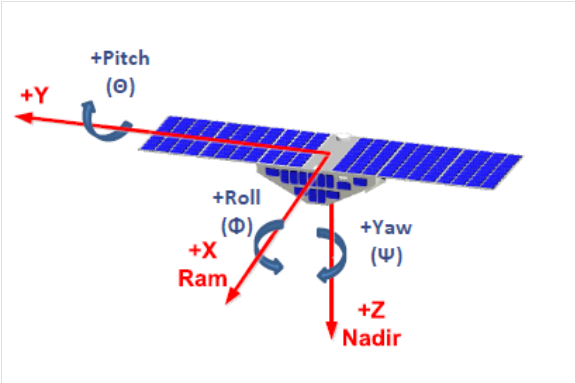

(a)CYGNSS body frames

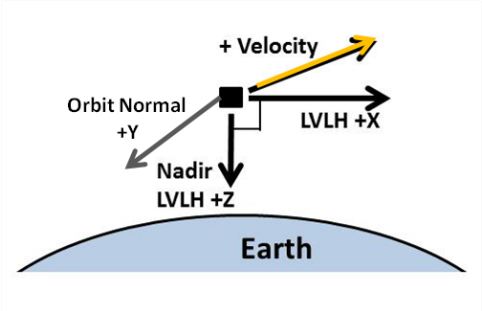

(b)LVLH reference frame convention

Figure 1. CYGNSS with body reference coordinate frames and LVLH reference frame convention

craft and enter into Sun Point configuration within 3 orbits after separation from the deployment vehicle and that it must be able to hold Sun Point with the magnetorquers, magnetometer, CSS and solar panel telemetry only. (The reaction wheel array, star tracker and GPS are not assured when the ADCS is in Sun Point mode.) Performance requirements during Sun Point mode stipulate that ADCS must hold the microsatellite zenith face Sun pointed to within 30° indefinitely.

These operations, mission and hardware availability requirements and constraints governed both the choice of the hardware as well as the design of the algorithms used by ADCS.

4. ADCS Hardware Selection

CYGNSS's suite of sensors available for attitude determination consists of 5 distinct sensors along with state data from the solar arrays; 2 sets of actuators are available for spacecraft attitude control. The sensor suite consists of a three-axis magnetometer; a single-headed star tracker; a 2-axis medium Sun sensor (MSS) mounted co-boresighted with the star tracker for operation during star tracker solar outages; and a zenith-deck mounted coarse Sun sensor (CSS) to aid in solar-pointing the solar arrays. A GPS receiver provides earth-relative position, velocity and time information which are further used to establish the instantaneous LVLH attitude reference. The ADCS actuator suite consists of three torque rods and a reaction wheel triad assembly (RWA) suitably oriented to ensure that the central pyramidal axis is oriented along the microsat pitch rotation axis. Sensor and actuator performance parameters are not included in this paper because disclosure agreements with various vendors prohibit public release of these parameters at this point in time.

As mentioned earlier, different sensors and actuators are available for use in the LVLH based pointing mode (whether for nadir pointing or HDTEA aligned attitudes defined relative to the LVLH frame) compared with the non-LVLH modes (Rate Damp and Sun Point). Detumble uses only the magnetometer and the magnetorquers; Sun Point additionally uses the CSS and solar panel telemetry from the 3 faces $(\pm X, -Z)$. LVLH mode admits the use of all sensors and all actuators as it is CYGNSS's highest performance mode. The magnetometer, star tracker (or MSS during the star tracker's Sun outage periods) and GPS are the key attitude measurement sensors used in this mode. The reaction wheels are used to control micro-satellite attitude and the torque rods, to manage the wheel momenta.

5. ADCS System

The CYGNSS ADCS flight software system primarily consists of a mode manager, sensor and vehicle health and safety monitor, the attitude determination sytem (ADS) and the attitude control system (ACS). The ADCS mode manager manages the mode transitions for the ADS and ACS in response to overarching commands from the spacecraft mission manager and will not be detailed here. In a single string system such as CYGNSS, the fault detection and isolation (FDI) or the vehicle health and status monitor (VHSM) systems primarily monitor signals and look for probable errors and caution conditions which they flag for ground control and the spacecraft mission manager. Neither of these functions are detailed in this paper where the focus is the ADS and ACS algorithms. Nevertheless the component block interconnection diagram shown in Fig. 2 defines the overall ADCS flight software and the context in which ACS and ADS operate within the ADCS flight software.

The ADCS mode manager coordinates and manages the transitions between the objective modes commanded by the spacecraft mission manager. Note that the CYGNSS ADCS mode manager separates out the mode commands to ACS and ADS thereby allowing for the possibility that the ACS and ADS can be in different modes. This is particularly necessary to allow the ADS Kalman filters to converge before the ACS acts on state estimates produced by an ADS still undergoing transient effects before convergence. The mode manager commands ACS and/or ADS one of four possible modes, the three key of which have already been mentioned previously : Rate Damp, Sun Point, LVLH, and Standby. Standby is a hold mode wherein the ACS and ADS will merely hold their values associated with their prior state and is akin to a free-drift mode.

The entire ADCS system operates at a 4 Hz update rate. All sensors are sampled and their most current readings reported by the spacecraft Command and Data handling System (CDS) to the ADCS at 4Hz along with the measurement time stamps. ADCS actuation commands to the reaction wheel array and torque rods are produced at 4 Hz and passed to the actuators.

ADS and ACS are largely distinct for Rate Damping, Sun Point and LVLH pointing modes. Rate Damping using mag-

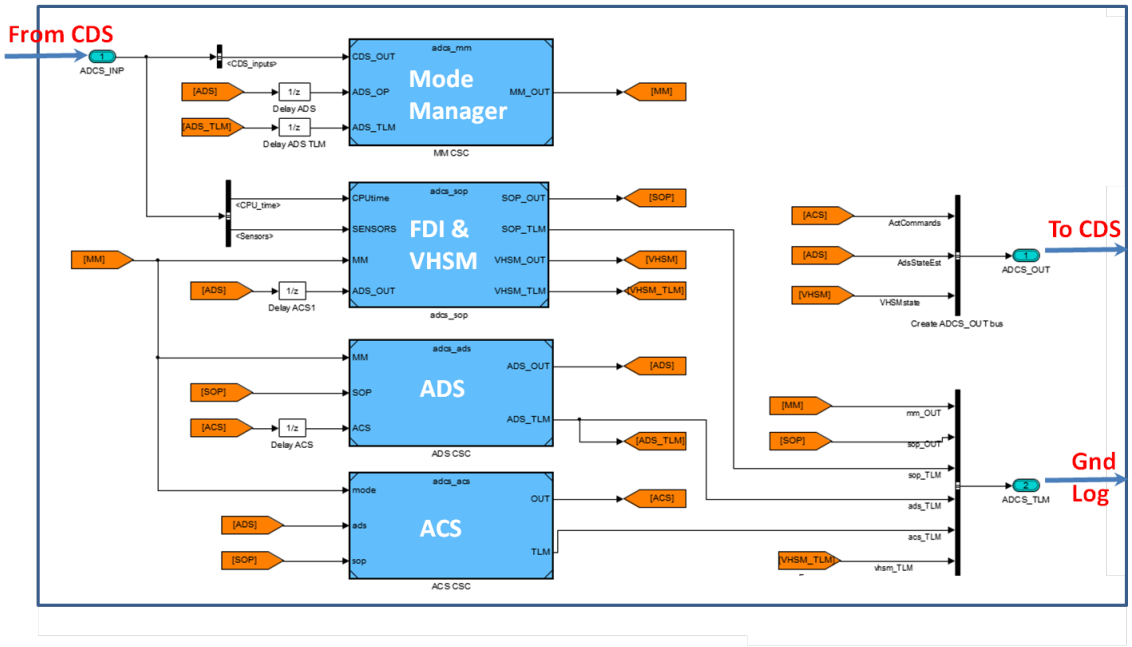

Figure 2. ADCS Architecture Diagram showing the ADCS Mode Manager, VHSM, ADS and ACS

netometers and magnetorquers is quite simply realised using the B-dot control law from the literature [4], [2] and both the ADS and ACS will be summarised here. The star tracker and magnetometer based extended Kalman Filter (EKF) used for the LVLH attitude determination and the reaction wheel based attitude error controller are also documented in the literature and the salient features of the EKF and the feedback controller are repeated here. The most complex of the ADCS modes is the Sun Point mode; details on the description of the CYGNSS approach to the spin-stabilised solar array based Sun Point controller are provided in greater detail in a companion paper by Shoer et. al. [5] and will only be briefly summarised here.

The ADCS mode manager accepts a desired ADCS mode command from the spacecraft Command and Data Handling system, and coordinates the entry of ACS and ADS into the desired mode based upon allowable transitions and acceptable conditions for transit of ACS or ADS such as acceptable spacecraft rates or estimation filter performance. The overall transition diagram is shown in Fig. 3.

In the overall concept of operations for CYGNSS, ADCS transitions into Sun Point mode upon detumbling the spacecraft after its initial separation from the deployment vehicle. Thereupon, the first priority is to locate the Sun using the zenith deck mounted single axis CSS and solar panel telemetry from CYGNSS's three faces equipped with the same. To perform Sun acquisition then, CYGNSS is put into a slow roll about its X-axis which holds its X-face fixed while barbequing the zenith deck. The Sun is declared found when input power registers on one or more faces corresponding to an incident angle of 60 degrees or larger. At that point, the slow roll is arrested and an eigenaxis slew negotiated to orient the zenith face towards this Sun vector. ADCS then exits the Sun Acquisition submode to prepare for its spin-stabilised Sun Hold submode; this it does by commencing a Z-axis (spacecraft principle-axis) spin. The conical scanning gradient search algorithm is the principle peak solar power finding algorithm used to track the Sun; this initiates which makes the Sun direction vector an observable in the micro-satellite body frame and allows a control policy tracking the peak power gradient to admit actuation towards the Sun. Once the Sun has been acquired such that the -Z-axis is locked on to it, the principle axis spin ensures that this Sun vector can be held with very low effort.

Transitioning from Sun Point to any LVLH relative attitude to commence HDTEA or nadir pointing operations means that the mode manager must first arrest the Sun aligned spin (done via a return to Rate Damp) and then, once spacecraft rates are sufficiently low, activate the LVLH attitude estimator. Once the filter is deemed to have converged, the mode manager commands ACS into its LVLH control mode which realises the commanded attitude. With this as background, the ex-postulation of the details of the ACS and ADS algorithms are provided in the next two sections.

6. Attitude Determination System

The CYGNSS attitude determination system (ADS) has two primary estimation modes : Rate Damp, and LVLH. When ADCS and hence the ACS are in Sun Point mode, ADS remains in Rate Damp mode to perform the same rate estimation as it perfomed to detumble the spacecraft. Consequently, there is not a distinct Sun Point ADS mode. The algorithms used in each mode are summarised below.

Rate Damp ADS - Rate Estimator

Sun Point mode involves spinning the spacecraft about a desired axis - the roll axis during the early part of Sun acquisition, a eigenaxis to tumble the zenith face normal towards the Sun vector, and then a principle axis spin-up. All these operations rely on an estimation of the spacecraft rate. In the absence of a true inertial rate measurement unit, CYGNSS relies on rate estimation using the magnetometer via the magnetometer-based rate estimation EKF developed in [6]. During detumble, the rate estimates of the spacecraft are used to form B-dot. For detumble, the rate estimation filter is more

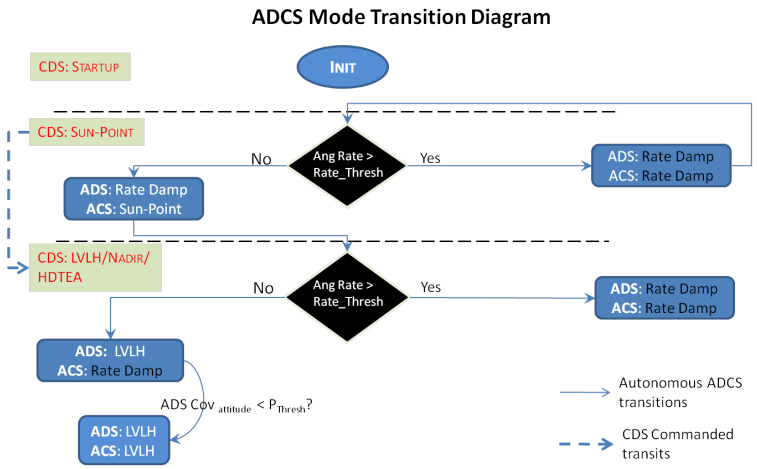

Figure 3. ADCS Mode Transition Diagram. Commands from CDS are mode change commands from the Spacecraft Primary Mission Manager to the ADCS system. ACS and ADS modes are sequenced and transitioned in stages in response to CDS directives.

complex than the simple back-difference and low-pass filter on B-field measurements conventionally performed, but it tends to show much better performance with a better estimate of magnetic field rate $\dot{\hat{b}}$.

Any extended kalman filter consists of three key steps: state and covariance propagation, gain matrix computation and covariance update and finally, measurement-based state updates. These rely on onboard models of the dynamics (rate) and measurement models with companion uncertainty models which are integrated and linearised as the case may be, about the current best estimates.

The kinematics of the magnetic field measurement is popularly expressed in the body frame as $\dot{b}_B = -\omega \times b_B$; this assumes that the inertial rate of change of the Earth's magnetic field is negligibly small over small intervals of time and therefore all observed magnetic field rates are due to body rates relative to inertial. The filter states estimated in this EKF are the spacecraft angular rate and the magnetic field: $x = [\omega^T, b^T]^T$. Since the only direct sensor measurement is the magnetometer, the measurement equation then is $y_k = b_k + v_k$ with v_k the the magnetometer measurement noise.

The nonlinear dynamic equations used in the rate estimation filter with the above states then capture the spacecraft rate dynamics and the magnetic field models as:

$$\dot{\omega} = J^{-1}(-\omega \times (J\omega + h_{rw}) + q^{mtq} \times b) + w_1 \quad (1)$$

$$\dot{b}_b = -\omega \times b + w_2 \quad (2)$$

where J is the spacecraft inertia tensor in the body frame, h_{rw} the stored momentum in the reaction wheels, and q^{mtq} the magnetorquer dipole in the body frame. w_1, w_2 are zero-mean, white, Gaussian process noise with noise spectral density that must capture modeling error terms such as unmodelled disturbanced torques, inertia uncertainties and unmodeled drift in the inertial magnetic field which was ignored when the magnetic field rate was so simply rendered as a function of the micro-satellite rate only. Based on the previous best estimates of ω and b at time $t = t_{k-1}$, the above equations are used to *predict* the state at the current time t_k. This predicted state is denoted $\hat{x}_k^-$.

As in any EKF, the above equation is used to predict the rates at the current time based on the last best estimate of the filter states. The prediction errors are then estimated by a Kalman Filter via simple linearisation of the above dynamics about the current predicted states. The Jacobian used to formulate the linearised dynamics for the above nonlinear dynamics models is used to both propagate the measurement error covariance matrix and form the estimator gain matrix to correct the state and covariance predictions and thus compose their updated estimates. The continuous time state and measurement Jacobian matrices are simply given by:

$$\begin{aligned} F_{t_k} &= \begin{bmatrix} \frac{\delta\dot{\omega}}{\delta\omega} & \frac{\delta\dot{\omega}}{\delta b} \\ \frac{\delta\dot{b}}{\delta\omega} & \frac{\delta\dot{b}}{\delta b} \end{bmatrix}_{t=t_k} \\ &= \begin{bmatrix} J^\dagger(S(J\omega_k + h_{rw}) - S(\omega_k)J) & J^\dagger S(q_k^{mtq}) \\ S(b_k) & -S(\omega_k) \end{bmatrix} \\ y_{t_k} &= \begin{bmatrix} \frac{\delta y}{\delta\omega} & \frac{\delta y}{\delta b} \end{bmatrix} \\ &= \begin{bmatrix} 0_{3x3} & I_{3x3} \end{bmatrix} [\omega_k^T, b_k^T]^T \end{aligned}$$

where $J^\dagger = J^{-1}$, $S(\xi)$ represents the skew operator $\xi\times$ for vector ξ. Given that the propagation and updates must be computed at discrete points in time while the above state dynamics matrices are expressed in continuous time form, the associated state transition matrix is necessary. Recognising that for a nonlinear, time-varying system, the propagation dynamic model can be written as: $\dot{\Phi}_k = F_k\Phi_k$, from which both the state dynamics predictions as well as the state transition matrices are computed with a 4^{th} order Runge Kutta integrator. With Φ_k in hand, the covariance matrix propagation and Kalman filter gain equations are computed according to conventional Kalman Filter implementation guidelines:

$$P_{k+1}^- = \Phi_k P_k^+ \Phi_k^T + Q_k \quad (3)$$

$$L_k = P_k^- H_k^T (H_k P_k^- H_k^T + R_k)^{-1} \quad (4)$$

where Q_k is the process noise model. The state and filter updates are performed based on the current measurement matrix, the gain matrix and most recent measurements. These equations expressed in the Joseph form for robustness are

given by:

$$P_k^+ = (I - L_k H_k) P_k^- (I - L_k H_k)^T + L_k R_k L_k^T \quad (5)$$

$$\hat{x}_k^+ = \hat{x}_k^- + L_k(y_k - H_k \hat{x}_k^-) \quad (6)$$

The ADS estimates output to the controller consist of $\hat{\omega}_k$ and $\hat{b}_k$ contained in $\hat{x}_k^+$. Additionally, because the Rate damping and Sun Point controller regulates rate via the B-dot control law, the estimator also outputs $\dot{\hat{b}}_k = \hat{b}_k \times \hat{\omega}$.

LVLH Attitude Estimator

The LVLH attitude estimator is a conventional attitude estimator based on attitude measurements from a star tracker, a 2-axis Sun sensor and a magnetometer. The basic elements of an EKF having already been defined, this section defines the critical state dynamics and measurement equations only. The essentials of the LVLH EKF are summarised in the block diagram in Fig. 4

Given that attitude and not just attitude rate estimation is performed in this step, the key dynamics equations used in the attitude estimation filter are:

$$\dot{\mathbf{q}} = \Omega \mathbf{q} \quad (7)$$

$$\dot{\omega} = J^{-1}((-\omega \times (J\omega + h_{RW}) + T_{ext}) + m_{bias} \quad (8)$$

$$T_{ext} = \tau_{RW} + (q^{mtq} \times b) + G\hat{G} \quad (9)$$

$$\dot{m}_{bias} = 0 \quad (10)$$

where attitude is captured as the unit attitude quaternion $\mathbf{q}$, T_{ext} represents the known predictions of the external torques exerted on the micro-satellite including the applied reaction wheel torques, the magnetorquer-induced applied torque computed from the commanded dipole moment effected in the magnetic field measured at the instant in time, and the gravity gradient torque at that spacecraft attitude in the Earth gravitation.

The unknown residual torque bias is represented by m_{bias} and comprises an additional state vector to the filter. Further states augment this filter representing the unknown magnetometer and MSS mounting misalignment errors. Collectively then, the LVLH mode attitude estimation filter consists of the following error states: attitude quaternion error, rate error, torque bias, magnetometer mounting misalignment, MSS mounting misalignment.

The process of linearising the plant dynamics to express the state transition, covariance and gain matrices are the same as outlined previously from the above set of models and are not repeated here. The measurement equations, however, will be defined for each sensor.

The magnetometer measurement model is based on the derivations provided by the work of Martel and Psiaki [7]. This theory expresses the magnetic field measurement equation as $b_k = b_{k.mdl} + \frac{\tilde{b}_b \times \hat{b}_b}{\|\tilde{b}_b\| \|\hat{b}_b\|}$ where $b_{k.mdl}$ is the value predicted by the onboard model of the Earth magnetic field at the position, velocity and time (typically as measured and reported by the GPS sensor); $\tilde{b}$ is the measured value of the magnetic field as reported by the magnetometer and $\hat{b}$ is the best estimate of the field predicted by the filter at that point in time. The term on the right then expresses the measurement error residual. The measurement matrix for the magnetometer is derived by linearisation as:

$$H_{mag} = \begin{bmatrix} \frac{(\hat{b}^T \tilde{b}) I_3 - \hat{b}\tilde{b}^T}{\|\tilde{b}\| \|\tilde{b}\|} & \mathbf{0_3} & \mathbf{0_3} & \mathbf{0_3} & \mathbf{0_3} \end{bmatrix} \quad (11)$$

Note $\mathbf{0_3}$ represents the $3\mathbf{x3}$ zero matrix.

The 2-axis medium Sun sensor measurement gives a unit vector to the Sun in the spacecraft body frame. The associated measurement model can be articulated similarly from a measurement residual of the form: $\tilde{r}_{Sun} \times \hat{r}_{Sun}$ yielding a measurement matrix for the Sun sensor obtained by linearising the above equation as:

$$H_{mss} = \begin{bmatrix} ((\hat{r}_{Sun}^T \tilde{r}_{Sun}) I_3 - \hat{r}_{Sun} \tilde{r}_{Sun}^T) & \mathbf{0_3} & \dots & \mathbf{0_3} \end{bmatrix} \quad (12)$$

The Star tracker directly reports an attitude measurement; attitude measurement residuals are collated as a simple quaternion error of the form: $\delta q = \tilde{q}_b^I \otimes (\hat{q}_b^I)^{-}1$ which yields a measurement of the form:

$$H_{st} = \begin{bmatrix} I_3 & 0_3 & 0_3 & 0_3 & 0_3 \end{bmatrix} \quad (13)$$

Given the individual sets of measurements, an overall cascaded filter architecture is used to implement this sequence of measurements to update the attitude estimates at measurement time t_k. This architecture is shown in Fig. 4.

The first block called the SOP is not described here, and comprises a part of the ADCS flight software that is responsible for monitoring the quality of incoming sensor data for stale, unreasonable or out-of-range measurements. Note that the filter updates the attitude estimates separately from each sensor. The advantage of this approach is that it keeps the size of the measurement matrix and thus the gain matrix considerably smaller than if all sensor measurements were collated into a single vector and the full state vector were updated at once. As a result, this approach tends to be numerically more stable as it keeps the dimensions of the matrices being manipulated low.

7. ATTITUDE CONTROL SYSTEM

The ACS is designed to control the spacecraft to realise detumble, achieve Sun pointing and Sun holding with limited quality feedback, and to hold many LVLH relative attitudes such as aligning the nadir deck with the nadir (down) direction and acquiring and holding HDTEA, including a range of others. The Rate Damp, Sun point and LVLH mode control laws are vastly distinct algorithmically and thus the approaches will be defined hereby.

Rate Damping ACS

ADCS performs Rate Damping both upon entry and exit from Sun Point mode such as after initial deployment when it must detumble the spacecraft before Sun pointing the spacecraft. Rate damping is achieved using the magnetorquers using a straightforward application of the b-dot control law popularly used with magnetometers and magnetorquers [2], [4], [8]. The control architecture is simply:

$$q_{des}^{mtq} = R_b^{mtq} K_{mag} \frac{\dot{\hat{b}}_k}{\|\hat{b}_k\|^2} \quad (14)$$

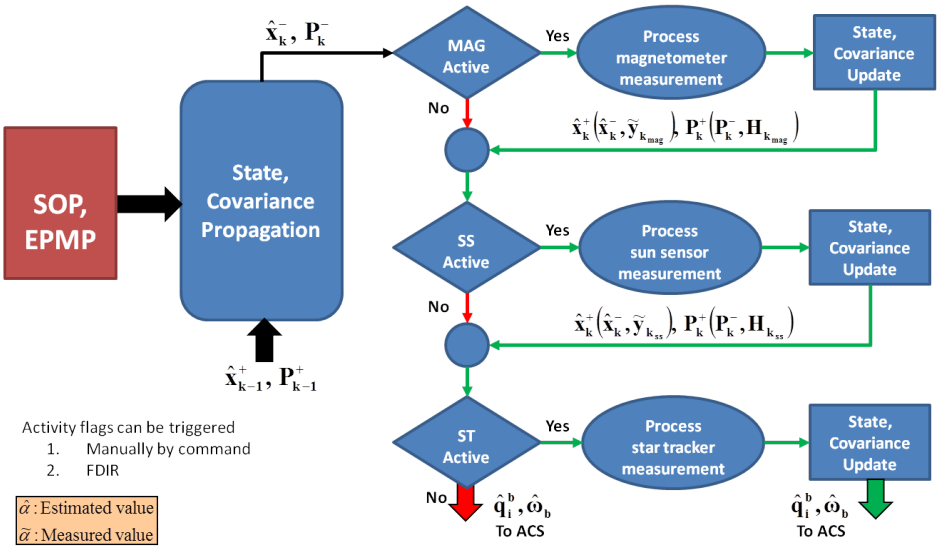

Figure 4. LVLH EKF operational sequence

where q_{des} is the desired computed control dipole moment which constitutes the command to the magnetorquer pulse-width modulators. R_b^{mtq} is the constant rotation between the body frame, in which the magnetic field and rate measurements are being reported and the mounting frame of the magnetorquer assembly; K_{mag} is the rate damping control gain (proportional) applied to the reported magnetic field rate measured at the spacecraft. Additional saturation and limits checks are applied before the dipole moment command is sent to the torque rod pulse width modulators. The essential block diagram is depicted in Fig. 5.

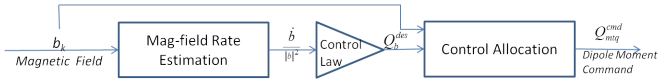

Figure 5. Rate Damping control architecture

The desired dipole moment is rotated into the torquer frame, limited to admissible torquer PWM saturation values, and scaled to ensure that the direction of the commanded moment is preserved upon limiting. These checks are performed in the control allocation block referred to in Fig. 5.

LVLH Relative ACS

The LVLH relative attitude controller is another simple state feedback attitude error regulator and consists of an *attitude control law* as a state error regulator, a *momentum manager*, and *control allocation logic*. A reference pointing attitude set-point q_{ref} defined in the LVLH frame is provided with a zero LVLH relative angular rate command. The instantaneous attitude error at time t_k is first simply computed from the unit quaternion difference operation, $q_e = q_{ref} \otimes q_k^{-1}$. Depending on the norm size of the pointing error, ACS defines itself to either be in a slewing or settling configuration. If the angular error is larger than a parametrically defined *pointing error threshold*, ACS is considered to be coarse pointing whereby it performs a rate control manoeuvre driving to a constant slew rate along the pointing error eigenaxis ξ, until the angular error is within the pointing error threshold. At that point, it switches to its fine pointing state whereby it *settles* from the rate controlled slew to capture the desired pointing attitude.

The attitude control law is a simple PID-like law with state

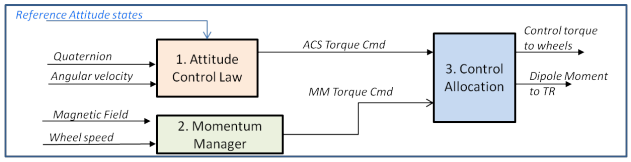

Figure 6. LVLH state feedback attitude and attitude controller

feedback linearisation compensation as summarised below with the key operational elements defined in Fig. 6.

$$\text{Slew:}\quad \tau_{des}^{att} = K_w\omega_e + (\hat{\omega}_k \times (J_{sc}\hat{\omega}_k + h_{rw})) \quad (15)$$

$$\text{Settle:}\quad \tau_{des}^{att} = K_w\omega_e + K_q q_{error} + K_i \int (q_{error})dt + (\hat{\omega}_k \times (J_{sc}\hat{\omega}_k + h_{rw})) \quad (16)$$

where $\omega_e = \omega_{ref} - \hat{\omega}_k$ is the angular rate error and $q_{error} = q_{e,v} \cdot q_{e,s}$ is a globally regulating error compensation formulation of the 4-element quaternion error vector. The computed compensation torque varies depending on whether the ADCS is attempting to perform a rate capture or attitude capture (slew or settle options). $q_{e,s}, q_{e,v}$ represent the scalar and vector components of the quaternion error relative to the desired attitude. The terms in the control law above, it can be seen, consist simply of the attitude error driven terms and the feedback linearisation augmentation to cancel the Eulerian momentum-based gyroscopic term.

The momentum manager is a simple proportional controller on the reaction wheel momentum vector for the three wheel array. The CYGNSS spacecraft operates its reaction wheels about a momentum bias so the wheel momentum error vector is computed relative to the desired momentum bias defined as a set-point. Note that momentum management is only performed when ACS is in its Settle sub-mode; in the transient Slew mode, it is inevitable that the wheels must necessarily change their stored momenta to either spin up or spin down the spacecraft hence momentum management in this period is not performed

$$\text{Slew:}\quad \tau_{des}^{mm} = 0 \quad (17)$$

$$\text{Settle:}\quad \tau_{des}^{mm} = K_{mm}(h_{bias} - h_{rw}) \quad (18)$$

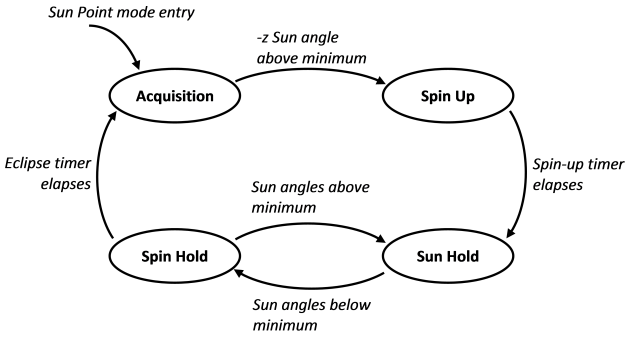

Figure 7. ACS submodes used to realise Sun Pointing from initial Sun finding to Sun holding through eclipse.

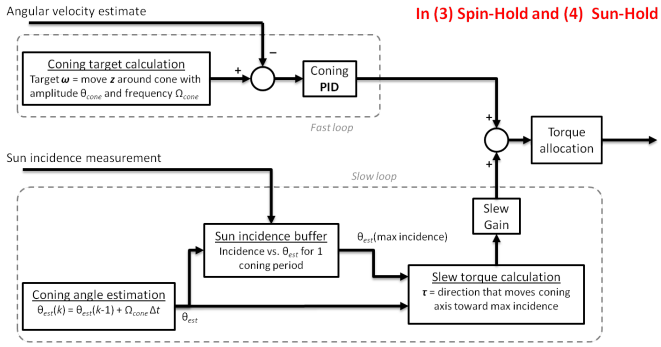

Figure 8. Inner (rate control) and Outer (gradient search for Sun direction) loop control architecture for Sun Point ACS

Finally, the actuation commands are assembled in the control allocation operation. The momentum-management torque realisable by the torque rods are computed by first computing the dipole moment using the vector triple product relationship, recognising that the magnetic torque vector relates dipole moment and an ambient magnetic field as $\tau_{mtq} = q^{mtq} \times \hat{b}_k$ and that the resulting torque would be orthogonal to the instantaneous magnetic field vector. The dipole moment commanded of the torque rods is then computed from the relationship as:

$$q^{mtq}_{cmd} = -R^{mtq}_{b} \frac{(\tau^{des}_{MM} \times \hat{b}_k)}{\hat{b}^T_k \hat{b}_k} \tag{19}$$

The expected torque on the body from the magnetorquer actuation can be predicted from the $\tau^{cmd}_{mm} = q^{mtq}_{cmd} \times b_k$ relationship. This torque is then negated from the command applied to the wheels to ensure that the effective actuation on the body is then identically, or very nearly so, to that required for attitude control.

$$\tau^{RW}_{cmd} = \tau^{att}_{des} - \tau^{mm}_{cmd} \tag{20}$$

Sun Point Control

Only the outline of the Sun Point controller method is provided here as specific details of the methodology and its convergence and stability properties are addressed in a companion paper [5]. The objective of the ADCS Sun Point mode is to find the Sun, orient and stably hold the micro-satellite solar panel face to within $30\,\mathrm{deg}$ of the Sun vector using solar panel telemetry from the $\pm X$ faces, the zenith deck-mounted CSS and the magnetometer for feedback information and actuation with the torque rods only. Key architectural elements of the Sun Point ADCS controller are shown in Fig. 7.

Sun acquisition and pointing proceeds in four Sun Point ACS submodes with transitions governed by timers and thresholds on measurements. The goal of this architecture is to be simple and robust, while maintaining necessary capabilities such as distinguishing between entry into orbit night and loss of Sun pointing. The submodes used to effect Sun Pointing are:

- Sun Acquisition
- Spin Up
- Sun Hold
- Spin Hold

Sun Acquisition initiates the overall Sun Point mode with the stated purpose to rotate the spacecraft from any arbitrary initial attitude so that the Sun is within the -Z coarse Sun sensor field of view. The Acquisition submode achieves this result by performing a slow roll of the spacecraft about its X-axis, a manoeuvre which, with the CYGNSS sensor geometry, is effectively a full-sky search for the Sun. The Sun is declared found when input power registers on a face corresponding to an incident angle of 60° or larger. At that point, the slow roll is arrested and an eigen-axis slew is negotiated to orient the zenith face towards this Sun vector.

When the Sun is within the -Z coarse Sun sensor field of view, the attitude control system transitions into Spin Up submode. As the name implies, the purpose of this submode is to establish an equilibrium spin about the spacecraft's major inertia axis: its Z-axis. The rate target is $1.5\,\mathrm{deg}/s$ (called the "coning rate" because of its effect on the coarse Sun sensor boresight) about the -Z body axis, with control error determined from the rate estimate; the target remains the same for all subsequent Sun Point submodes.

The conical scanning gradient search algorithm then initiates which makes the Sun direction vector observable in the micro-satellite body frame and allows actuation towards the Sun. A block diagram of the Sun hold inner-outer loop controllers is shown in Fig. 8.

Sun Hold submode is the key phase of Sun Point, with the goal of converging the spacecraft-to-Sun vector towards the spacecraft -Z axis. The Sun Hold algorithm is a gradient search that buffers received power measurements from the Sun sensors as all three boresights sweep out cones about the -Z axis. The flight software estimates the direction to the Sun from information contained in a rolling buffers, given assumptions and knowledge about the spacecraft rate, and computes the torque that will slew the main solar panel toward that direction. In effect, the spacecraft carries out a gradient search to home in on the direction of maximum received power on the solar array. Fundamentally, the control architecture used herein consists of two spectrally separate loops. A fast inner rate control loop merely tries to maintain the spin-rate about the -Z face. This it does as a simple proportional controller using the spacecraft rate estimate outlined earlier in Sec. 6 and comparing it with the desired spin rate. A slower outer loop uses solar panel (or CSS) power information collected in the rolling buffer to identify the direction (in the body frame) of peak power seen by the CSS. The peak-power direction in the spacecraft X-Y projected axis defines the direction in which the body Z-axis must be tipped. A two degree-of-freedom proportional controller regulates the pointing error of the zenith face normal to ensure

that the zenith face stays Sun pointed. This controller is quite simply a classic design of an *extremum seeking control* law; at any instant in time, the gradient search controller forces the spacecraft to move in the direction of the peak-power. Equilibrium is ensured when over the entire 360° circulation, the power collected by the CSS is identical.

It is for this reason, incidentally that the spin direction and the signal (power) collection axis must be offset; we accomplish this on CYGNSS by canting the CSS from the zenith deck by some offset angle (about 10° in a known sense). In this way, the spin-axis is allowed to be an equilibrium spin axis of the spacecraft which admits low control effort to hold the spin direction whilst the canted Sun sensor provides the observability to the extremum seeking logic.

If the current generated by all the solar panels falls below a threshold value while in Sun Hold, then the ADCS assumes that the spacecraft has orbited into Earth eclipse. It transitions into Spin Hold submode, which simply controls the spacecraft angular velocity to the nominal spin. The Spin-Hold submode basically effects the faster inner coning rate loop only which just tries to maintain the spin rate based on the magnetometer-based rate estimation only. A timer also increments in Spin Hold submode; if the elapsed time is greater than the expected length of eclipse then the attitude control system treats the situation as a loss of Sun pointing and restarts Acquisition submode. However, if sunlight comes back onto the sensors at any moment before the timers elapse, then the ADCS returns to Sun Hold submode and the gradient search. The vehicle will then re-converge from any small loss of pointing that may have occurred during the eclipse. Apart from the timers and the specific submode transition logic, the attitude determination and control in Spin Hold is identical to that in Spin Up submode.

8. ADCS PERFORMANCE

CYGNSS's ADCS predicted performance is being verified based on extensive simulations in high fidelity simulators prior to its anticipated launch late in 2016. Results based on simulations are included below for performance in various modes.

Rate Damping

At a minimum Rate Damping will be necessary upon separation from the deployment module post-launch to detumble and capture the spacecraft. The performance of the magnetometer-based Rate Damp filter to estimate spacecraft rates and the ability of the ACS to capture and stabilise the spacecraft from an initial rate of about $5\,\mathrm{deg}/s$ are shown below in Figs. 10 and 9. Note that Fig. 10 focusses on the detumble phase of the flight and is therefore a subset of the full performance depicted in Fig. 9.

Simulation-based results in Fig. 10 show the CYGNSS spacecraft in a post-separation spin in its stowed configuration with associated mass properties and initial angular rate of $5\,\mathrm{deg}/s$ about an arbitrary body axis. The Rate Damp mode angular rate and magnetic field rate (B-dot) estimator, and the B-dot controller capture the spacecraft, reducing its angular rate to less than the objective value of $0.5\,\mathrm{deg}/s$ root-mean squared in about 1.3 orbits. The performance of the estimator is shown via the angular rate estimation error statistics with the associated rate filter standard deviation (square root of the covariance).

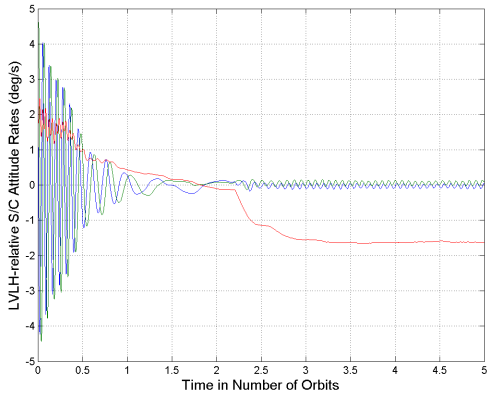

Figure 9. Spacecraft true body rates after initial deployment from Rate Damp through Sun Pointing. After detumbling for about 2.25 orbits, the spacecraft commences Sun Point, targeting a body yaw spin rate of $1.5°/s$. The tracks show the X (in blue), Y (in green) and Z (in red) components of angular rates. Note that the Z yaw rate settles out at about $1.5°/s$ as desired for Sun Point operations, at about 2.5 orbits.

Sun Pointing

Upon successfully detumbling when the spacecraft body rates have dropped to below certain threshold values, the spacecraft transitions in to Sun Point mode which, as detailed above, involves first a Sun acquisition phase then followed by a -Z principle axis spin which renders the Sun line-of-sight vector observable; the Sun Point controller produces torque commands (via the magnetorquers) to enable the spacecraft spin axis to track the Sun vector such that the principle axis of spin is locked onto the Sun direction while the body rotates at the desired coning rate of $1.5\,\mathrm{deg}/s$ about this axis as shown in Fig. 9.

Key results showing the Sun angles between the solar array faces or Coarse Sun Sensor with the Sun within the context of the Sun Point operation are included in Fig. 11. Angles between the zenith deck mounted Coarse Sun Sensor and the Sun vector are shown in Fig. 11-A starting from detumble operations in Rate Damp mode. After detumble, the Sun Point controller steps through its Sun point sequence and the corresponding Sun angles to the three solar array faces during this phase are also shown in Fig. 11-B. The CSS is angled relative to the zenith deck accounting for an approximately $10°$ bias value between its boresight axis and the Sun vector. The coning-based controller tracks the Sun with an about $5°$ precision about this offset angle.

These results are all produced for the micro-satellite in its stowed solar panel configuration. The transition into the deployed array configuration occurs after this phase, and is not included in these results.

LVLH Relative Pointing

In LVLH modes, an LVLH frame relative pointing attitude is commanded by CDS (spacecraft mission manager). These attitudes might be Nadir pointed whereby the spacecraft body frame must be aligned with the LVLH reference frame at all times to accuracies and tolerances specified in the requirements, they might be in the High-Drag TEA where a high pitch angle is to be realised and maintained, or they might be in any intermediate attitude relative to the LVLH frame as

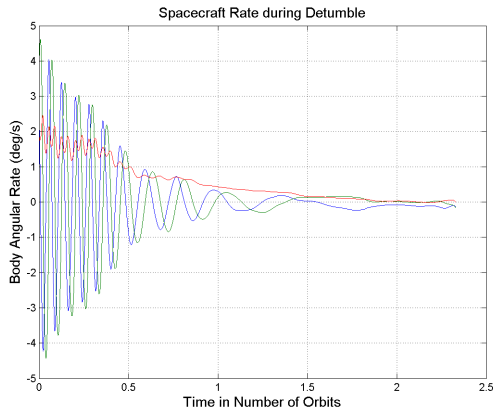

(a)Rate Damp Control Performance

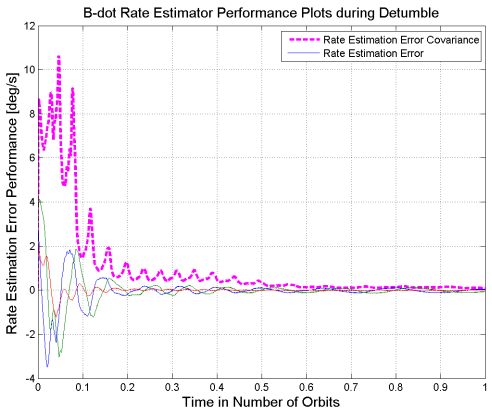

(b)Rate Damp Estimator Performance

Figure 10. Rate Damping performance for CYGNSS with initial post-separation spin rate of $5\,\mathrm{deg}/s$. Subplot (a) shows the controlled system performance stabilising the spacecraft. Subplot (b) shows the estimator performance for this single run bounded by the filter-estimated standard deviation focussed over the first orbit during the early convergence phase. The filter states remain similarly bounded through the performance interval once it has converged.

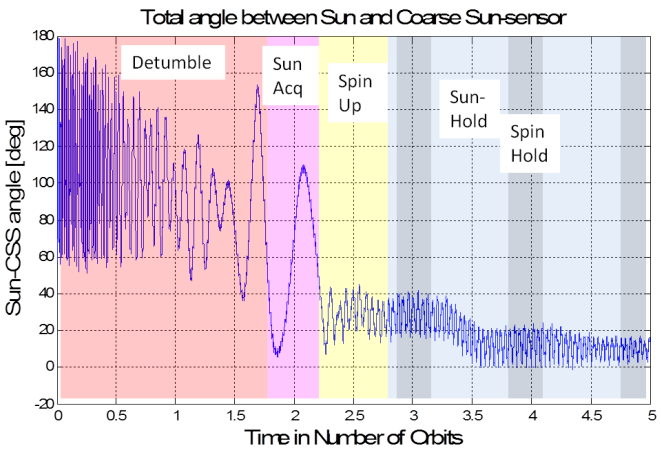

(a)Coarse Sun Sensor Angles to Sun in Sun Point sequence

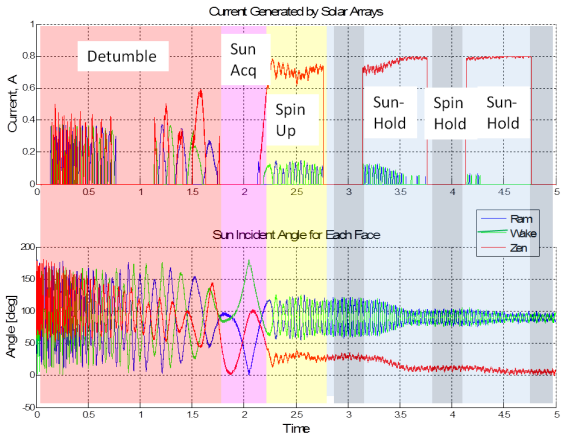

(b)Solar Array Collection Current

Figure 11. Subplot (a) shows the angles between the zenith face Coarse Sun sensor and the Sun during detumble through the Sun point sequence. The Sun Point controller stablises the zenith face on the Sun to within 7.5° in this simulation. The CSS is canted at an angle of 10° to the -Z face, resulting in the 10° bias seen in the CSS' mean angle to the Sun in the plot. Subplot (b) shows that the Sun vector stabilises onto the Zenith face to within $< 9^\circ$ stability cone in this scenario.

specified in the reference quaternion set-point.

Some examples of pointing performance during the LVLH modes are shown in Fig. 12. Results show the spacecraft in an initial LVLH aligned Nadir hold attitude for two orbits. At this point, the spacecraft mission manager commands ADCS to transition into the HDTEA high-pitch angle attitude which is merely a different attitude set-point in ADCS' LVLH mode. The transition occurs smoothly and quite rapidly. Plots show both the true and estimated euler angles relative to the orbit referenced LVLH frame.

A quick study of the attitude plots show that once in every orbit the attitude estimate appears to "bobble" for a short duration. These once per orbit "bobbles" are associated with the loss of the star tracker due to a Sun outage expected in its orbit. The Sun outage lasts about 20 minutes and the estimator must ride through the outage using aiding from the magnetometer and 2-axis medium Sun sensor (when available) only. However, since the MSS has a field of view that does not quite span the star trackers star tracker's Sun outage cone, the attitude estimator has periods where it must rely on the much less accurate magnetometer only. Per axis attitude estimation error in Nadir Point attitude degrades to about 1.9° (maximum value) during the Sun outage periods.

9. Conclusions

Eight CYGNSS spacecraft observatories are being designed and built to operate in a constellation in low inclination low-Earth orbits to facilitate continuous, gap-free tropical weather monitoring and forecasting. All on-orbit control of the spacecraft including post-launch stabilisation from deployment rates, Sun point capture and hold, and initial environmental drag-based orbital insertion are to be performed by the

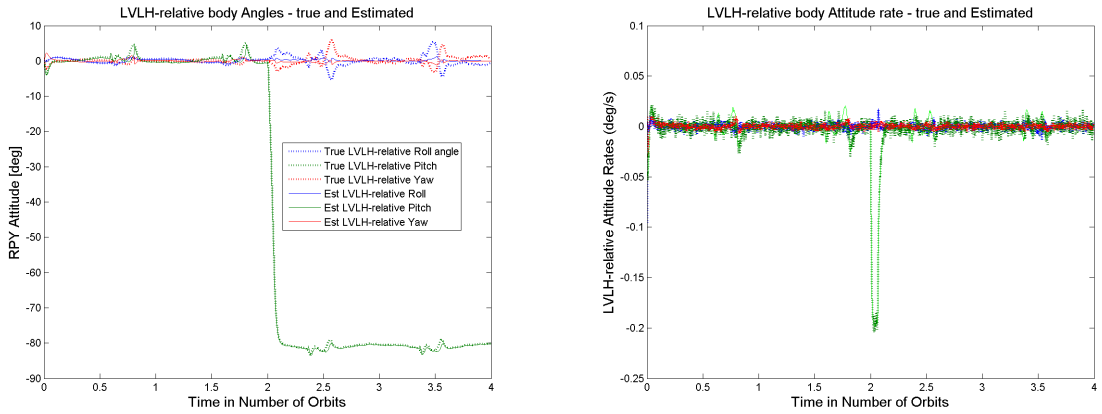

(a)LVLH relative RPY Euler Angles

(b)LVLH relative angular rates

Figure 12. LVLH angle and rate tracking performance. Subplot (a) shows the true and estimated LVLH relative body attitude expressed as Euler angles through Nadir Pointing, through the transition to HDTEA at the 2-orbit mark. Subplot (b) shows the body angular rate estimates (also relative to the LVLH rate) overlaid on true rates Solid lines mark the true values while the dotted show the estimates. The large pitch rate excursion at the 2-orbit mark is associated with the spacecraft slew from the Nadir Pointed attitude to the high-drag large pitch attitude.

CYGNSS attitude determination and control system, as is the long-duration attitude determination and control during the observatory's weather monitoring and Science data collection phase. This paper described the ADCS sensor and actuator suite selections, and the Attitude Determination and Control (ADS and ACS) software and algorithm designs for all modes of the on-orbit spacecraft operations specifically, Rate Damp (for detumble and rate capture) using magnetic field based sensors and actuation only; Sun Point using a single-axis Sun sensor for Sun vector determination and a spin-stabilised design to lock on and hold the Sun direction in a dynamic equilibrium state using magnetorquers for actuation; and LVLH hold for all star tracker aided 3-axis attitude determination and control operations using reaction wheels to control the spacecraft and magnetorquers to manage the momenta stored in the wheels about a biased (non-zero spin-rate to thwart excessive speed zero-crossings) value. Simulation results show that performance of the ADCS designs satisfactorily meet all performance and operating requirements.

REFERENCES

[1] C. Ruf, "Cygnss: Enabling the future of hurricane prediction," *IEEE Geoscience and Remote Sensing Magazine*, vol. 1, no. 2, pp. 52–67, 2013.

[2] B. DeKock, D. Sanders, T. VanZwieten, and P. Capo-Lugo, "Design and integration of an all-magnetic attitude control system for fastsat-hsv01's multiple pointing objectives," in *34th Annual AAS Guidance and Control Conference*, Breckenridge, CO, 2011.

[3] H. Steyn, Y. Hashida, and V. Lappas, "An attitude control system and commissioning results of the snap-1 nanosatellite," in *Proceedings of the 14th Annual AIAA/USU Conference on Small Satellites*, Logan, UT, 2000.

[4] J. Wertz, *Spacecraft Attitude Determination and Control*. D. Reidel, 1980.

[5] J. Shoer, L. Singh, and T. Henderson, "Conical scanning approach for sun pointing on the cygnss microsatellite," in *IEEE Aerospace Conference*, Big Sky, MT, 2015.

[6] C. Pong and D. Miller, "Angular rate estimation from geomagnetic field measurements and observability singularity avoidance during detumbling and sun acquisition," in *AAS Guidance and Control Conference*, Breckenridge, CO, 2013.

[7] F. Martel, P. Pal, and M. Psiaki, "Active magnetic control system for gravity gradient stabilised spacecraft," in *Proceedings of the 2nd Annual AIAA/USU Conference on Small Satellites*, Logan, UT, 1988.

[8] D. Vallado, *Fundamentals of Astrodynamics and Applications, 4th ed.* Microcosm Press, 2013.

Matthew Fritz *has a B.S. and M.S. degrees in Aerospace Engineering from the University of Texas, Austin where he focussed on estimation theory and in particular translational and attitude navigation solutions for spacecraft.*

Joseph Shoer *received a B.A. in physics from Williams College in 2006 and a Ph.D. in aerospace engineering from Cornell University in 2011, where he researched magnetic spacecraft actuator technology and novel attitude control algorithms for multibody satellites. He worked in the guidance, navigation, and control group of the Lockheed Martin Space Systems Company commercial satellite division before joining Draper Laboratory in late 2013.*

Leena Singh *has a B.S. in Physics and Mathematics and M.S. and Ph.D. degrees in Electrical Engineering with a concentration in Control Systems Theory where she focussed on the autonomous control of robotic, unmanned air vehicles. She has been at Draper Laboratory since 2001 where she is currently the group leader of the Strategic and Space Guidance and Control group. Leena Singh is an Associate Fellow of the AIAA.*

Timothy Henderson *has BS and MS degrees in Civil Engineering and has been involved in the development of spacecraft GN&C systems at Draper Laboratory for over 35 years. He is a Distinguished Member of the Technical Staff at the Draper Laboratory and currently a member of the Systems Engineering and Analysis Division acting as a systems engineer and program manager for several small spacecraft programs.*

Randy Rose *is a staff systems engineer for SwRI Space Systems Division where he serves as lead for spacecraft systems development. He has more than 34 years of experience in the spacecraft development community with experience in all aspects of spacecraft development including project management, systems engineering, computer architecture, ADCS, hardware and software design, I&T, and operations. His experience includes hands-on hardware development experience with all spacecraft subsystems. Mr. Rose is the NASA CYGNSS Project Systems Engineer responsible for the development of the overall CYGNSS system and microsat designs.*

Chris Ruf *received the B.A. degree in physics from Reed College, Portland, OR, and the Ph.D. degree in electrical and computer engineering from the University of Massachusetts, Amherst. He is currently a Professor of atmospheric, oceanic, and space sciences and Director of the Space Physics Research Laboratory at the University of Michigan, Ann Arbor. He has worked previously at Intel Corporation, Hughes Space and Communication, the NASA Jet Propulsion Laboratory, and Penn State University. In 2000, he was a Guest Professor with the Technical University of Denmark. He has published in the areas of satellite microwave radiometry and atmospheric, oceanic, land surface and cryosphere retrieval algorithms. Dr. Ruf is a member of the American Geophysical Union (AGU), the American Meteorological Society (AMS), and Commission F of the Union Radio Scientifique Internationale. He has served on the editorial boards of AGU Radio Science, the IEEE Transactions on Geoscience and Remote Sensing (TGRS), and the AMS Journal of Atmospheric and Oceanic Technology. He is past Editor-in-Chief of TGRS. Dr. Ruf is the Principal Investigator of the NASA CYGNSS mission.*